Negative moment of inertia and rotational instability of gluon plasma

Victor V. Braguta, Maxim N. Chernodub, Artem A. Roenko, Dmitrii A. Sychev

Negative moment of inertia and rotational instability of gluon plasma

Victor V. Braguta,[1,2,*] Maxim N. Chernodub,[3,†] Artem A. Roenko,[1,4,‡] and Dmitrii A. Sychev[1,2,§]

[1] *Bogoliubov Laboratory of Theoretical Physics, Joint Institute for Nuclear Research, Dubna, 141980 Russia*
[2] *Moscow Institute of Physics and Technology, Dolgoprudny, 141700 Russia*
[3] *Institut Denis Poisson UMR 7013, Université de Tours, 37200 France*
[4] *Dubna State University, Dubna 141980 Russia*

(Dated: March 7, 2023)

Using first-principle numerical simulations of the lattice SU(3) gauge theory, we calculate the isothermal moment of inertia of the rigidly rotating gluon plasma. We find that the moment of inertia unexpectedly takes a negative value below the "supervortical temperature" $T_s = 1.50(10)T_c$, vanishes at $T = T_s$, and becomes a positive quantity at higher temperatures. The negative moment of inertia indicates a thermodynamic instability of rigid rotation. We derive the condition of thermodynamic stability of the vortical plasma and show how it relates to the scale anomaly and the magnetic gluon condensate. The rotational instability of gluon plasma shares a striking similarity with the rotational instabilities of spinning Kerr and Myers-Perry black holes.

arXiv:2303.03147v1 [hep-lat] 6 Mar 2023

Introduction. The moment of inertia I is a quantity that expresses the resistance of a physical body to angular acceleration around a certain axis. In thermodynamic equilibrium, all physical objects have positive moments of inertia implying that in order to achieve an angular acceleration, one needs to apply a torque [1].

A negative moment of inertia of a body would imply that its acceleration generates a torque itself as if the physical body has a negative mass. Impossible in thermal equilibrium, this effect can be achieved in non-equilibrium, open systems. In mechanics, the realization of a $I < 0$ system requires presence of an active component such as a motor [2]. In electronics, the relevant example is played by electrical negative-impedance converters identified as an active electric circuit with negative resistivity [3]. A negative moment of inertia can also be realized in rotating Casimir systems associated with negative vacuum energy [4–6]. In addition, the negativity of isothermal moment of inertia can be achieved in thermodynamically unstable systems such as rotating black holes [7–11].

In our paper, we show that the *rigidly* rotating gluon plasma possesses, in thermal equilibrium, a negative moment of inertia ($I < 0$) below the temperature

$$T_s = 1.50\,(10)\,T_c\,. \tag{1}$$

where T_c is the deconfining transition temperature in a non-rotating plasma. We call T_s the "supervortical temperature" since at $T = T_s$, the *rigidly* rotating plasma looses its moment of inertia, $I(T_s) = 0$, in a distant similarity with a superconductor which looses its resistivity at a certain critical temperature.

Rotating quark-gluon plasma (QGP) with temperatures around the supervortical temperature (1) is routinely produced in relativistic heavy-ion collisions. Such plasma can have exceptionally high vorticity of the order of $\omega \approx (9 \pm 1) \times 10^{21}\,\mathrm{s}^{-1} \sim 0.03\,\mathrm{fm}^{-1}c \sim 7\,\mathrm{MeV}$ [12]. The properties of vortical QGP can be probed via spin polarization of produced hadrons which provide us with an opportunity to confront theoretical methods with experimental results [13, 14]. Theoretical approaches to the thermodynamics of rotating QGP always assume a rigid rotation of the system, drastically simplifying analytical treatment [15, 16].

The global consensus on the phase diagram of rotating quark-gluon plasma is still lacking. The thermal transition from hadronic to the QGP phase is accompanied by the restoration of the chiral symmetry and the deconfinement of color. There is a general agreement in the community that the rigid rotation, according to all model estimates, should reduce the critical temperature of the chiral transition in the fermionic sector [17–23].

However, the situation with the deconfining transition is not clear: the rigid rotation should either drive plasma to the deconfinement phase [24–28] or, with another scenario, should not affect the system at the rotational axis, forming, at high vorticity, an inhomogeneous confining-deconfining phase (the inverse hadronization effect) [29]. While signatures of the inhomogeneity are seen in kinematic variables in numerical simulations of pure gluon plasma [30], the numerical first-principle simulations have also revealed that the bulk critical temperature of the deconfining phase transition grows with the increase of the angular frequency [31, 32]. Moreover, it turned out that gluons and fermions have opposite effects on the critical temperature in rotating systems. It seems that the gluon sector wins in this contest and the deconfinement as well as the chiral critical temperatures increase with the rotation [33].

Thus, the model-based analytical approaches and the first-principle numerical simulations of rigidly rotating gluon plasma do not match. To explore this puzzle deeper, we look, in our work, at the mechanical properties of the rotating gluon plasma.

Angular momentum and moment of inertia. A mechanical response of a thermodynamic ensemble to a rigid rotation with the angular velocity $\mathbf{\Omega}$ can be quantified in terms of the conjugated variable, the total

angular momentum $\boldsymbol{J}$ which includes orbital and spin parts. These quantities determine the relation between the energy $E^{(\mathrm{lab})}$ in the inertial laboratory frame and the energy in the co-rotating, non-inertial reference frame, $E = E^{(\mathrm{lab})} - \boldsymbol{J}\boldsymbol{\Omega}$ [1]. The angular momentum $\boldsymbol{J}$ can be expressed via either the energy E or the free energy $F = E - TS$ in the co-rotating frame:

$$\boldsymbol{J} = -\left(\frac{\partial E}{\partial \boldsymbol{\Omega}}\right)_S = -\left(\frac{\partial F}{\partial \boldsymbol{\Omega}}\right)_T , \tag{2}$$

where we used $dE = TdS - \boldsymbol{J}d\boldsymbol{\Omega}$ and $dF = -SdT - \boldsymbol{J}d\boldsymbol{\Omega}$.

The moment of inertia is a scalar quantity,

$$I(T,\Omega) = \frac{J(T,\Omega)}{\Omega} = -\frac{1}{\Omega}\left(\frac{\partial F}{\partial \Omega}\right)_T . \tag{3}$$

which fixes a relation between the angular momentum $\boldsymbol{J}(T,\Omega) = I(T,\Omega)\boldsymbol{\Omega}$ and the angular velocity $\boldsymbol{\Omega} = \Omega\mathbf{e}$ of rotation around a fixed axis $\mathbf{e}$. Thus, the basic thermodynamic quantities (2) and the moment of inertia (3) can be determined with the help of the free energy F in the co-rotating reference frame.

For simplicity, we start our discussion with a cylinder-shaped gluon plasma with a radius R, rigidly rotating with the angular frequency Ω around the symmetry axis. We consider slowly rotating gluon plasma implying the velocity

$$v_R = \Omega R , \tag{4}$$

at the boundary of the system to be non-relativistic, $v_R^2 \ll 1$.

As we work with a large system size, $R \sim$ (a few) fm, the condition of the slowness of rotation also requires that the angular velocity should be much smaller than the intrinsic QCD energy scale, $\Omega \ll \Lambda_{\mathrm{QCD}}$. Moreover, in the whole range of temperatures in our work, $T \simeq (1.0 \sim 2.0)T_c$, the boundary effects can also be neglected because the spatial thermal correlation lengths in the strongly interacting gluonic plasma at $T \gtrsim T_c$ are of the order of $\Lambda_{\mathrm{QCD}}^{-1}$ or shorter, while below T_c the correlations are governed by the glueball masses $M_{0^{++}} = 1.653(26)\,\mathrm{GeV}$ [34] which correspond to even shorter correlation lengths. These physical conditions (system size R, temperature range T, and rotational frequency range Ω) correspond to physical conditions of vortical plasma created at RHIC in noncentral relativistic heavy-ion collisions [12].

Thermodynamics and velocity at the boundary. Several theoretical approaches to rigidly rotating gluon plasma [14, 25] express its thermodynamic properties as a function of the angular frequency Ω, suggesting independence (or a mild dependence) of the thermodynamics on the size of the system perpendicular to the axis of rotation [25]. However, first-principle numerical simulations indicate that the size dependence is very pronounced [31, 32] (see also discussion in Ref. [19]). Moreover, it appears that the thermodynamics of the slowly rotating system can be expressed as a function of the velocity of the system at the boundary (4). This statement, valid at least in the $O(\Omega^2)$ order, implies that the thermodynamic variables incorporate angular frequency only via the common product ΩR [35].

Neglecting a shape change for the slowly rotating plasma, the moment of inertia can be taken as an Ω-independent quantity, $I = I(T,R)$.[36] Then, the thermodynamic relation (3) implies that

$$F(T,R,\Omega) = F_0(T,R) - \frac{1}{2}I(T,R)\Omega^2 , \tag{5}$$

where $F_0 \equiv F^{(\mathrm{lab})}(\Omega = 0)$ is the free energy of the non-rotating gas. The quadratic term Ω^2 has a minus sign in the co-rotating free energy (5) because this term represents a centrifugal energy responsible for particle runaway forces directed outwards of the axis of rotation.

For a classical system, the moment of inertia is determined by the mass (energy) distribution $\rho(T, x_\perp, \Omega)$, where $x_\perp$ is the radial coordinate normal to the axis of rotation. The effect of non-relativistic rotation on the uniform spatial mass distribution can be neglected, $\rho(T, x_\perp, \Omega) = \rho_0(T)$, implying that the moment of inertia takes the following familiar form:

$$I(T,R,\Omega) = \int_V d^3x\, x_\perp^2 \rho(T, x_\perp, \Omega) = \frac{\pi}{2}L_z R^4 \rho_0(T) , \tag{6}$$

where the integral is taken over the volume $V = \pi L_z R^2$ of the rotating cylinder.

While the derivation of Eq. (6) is valid for a non-relativistic rotation of a classical system, the system itself can be described by relativistic thermodynamics similarly to the gluon plasma where the relation (6) holds as well [37]. In this case, the quantity ρ_0, which determines the number of degrees of freedom that couple to rigid rotation, can have another origin. For example, ρ_0 in a Casimir system is negative so that the moment of inertia can take negative values as well [4, 5].

Combining Eqs. (5) and (6) we get that the co-rotating free energy can be expressed via the velocity v_R at the border of the cylinder $x_\perp = R$, given in Eq. (4):

$$F(T, v_R) = F_0(T,R)\Big(1 + \frac{1}{2}K_2 v_R^2 + O\big(v_R^4\big)\Big) , \tag{7}$$

where F_0 is the free energy in the absence of rotation. The response of the system with respect to the rigid rotation is represented in Eq. (7) by the dimensionless coefficient $K_2 = V\rho_0/(2F_0)$, where $V = \pi L R^2$ is the volume of the cylinder. The dimensionless moment of inertia K_2 relates the moment of inertia I to the free energy at a vanishing angular frequency, F_0 (notice that $F_0 < 0$):

$$I(T) \equiv \lim_{\Omega\to 0} I(T,\Omega) = -K_2(T)F_0(T)R^2 . \tag{8}$$

Thus, the angular frequency Ω enters the free energy (7) only as the velocity v_R at the boundary of the system (4).

Scale anomaly and equation of state. The free energy density, f, is determined via the scale (trace) anomaly [38]:

$$\langle T^{\mu}_{\ \mu}\rangle = -T^5 \frac{d}{dT}\left(\frac{f}{T^4}\right) . \tag{9}$$

Integrating (9), we get the free energy density:

$$f(T) = -T^4 \int_0^T \frac{dT'}{T'} \frac{\langle T^{\mu}_{\ \mu}\rangle(T')}{T'^4} , \tag{10}$$

highlighting the role of the anomaly $\langle T^{\mu}_{\ \mu}\rangle \neq 0$. When defining the integral in Eq. (10), we used the fact that the anomalous trace vanishes rapidly at low temperatures, $\langle T^{\mu}_{\ \mu}\rangle \sim \exp(-M/T)$, due to the mass gap $M \neq 0$.

The trace of the energy-momentum tensor $\langle T^{\mu}_{\ \mu}\rangle$ is computable in lattice simulations thus making it possible to calculate the free energy density (10) numerically from the first principles. However, this thermodynamically transparent expression can be rewritten in the lattice form which is more suitable for numerical computations [38]:

$$\frac{f(T)}{T^4} = -N_t^4 \int_{\beta_0}^{\beta} d\beta' \Delta s(\beta') , \qquad T = \frac{1}{N_t a(\beta)} , \tag{11a}$$

$$\Delta s(\beta) = \langle s(\beta)\rangle_{T=0} - \langle s(\beta)\rangle_T , \qquad s = \frac{S}{N_t N_z N_s^2} , \tag{11b}$$

where the $SU(N_c)$ lattice coupling $\beta = 2N_c/g_0^2$ is expressed in terms of the bare continuum coupling g_0, while the lattice action S will be specified below. In Eq. (11a), the lower integration limit β_0 is chosen in a deep confinement phase where the integrand, represented by the difference (11b) in the expectation values of the action at vanishing and finite temperature, is negligibly small.

The lattice formula (11a) has the same meaning as the continuum relation (10), with the right-hand-side of Eq. (11a) expressed via the lattice form of the scale anomaly. The latter includes the running coupling which is computable via the scale dependence of the lattice spacing $a = a(\beta)$.

The lattice form (11a) is also suitable for direct calculation of the free energy density f in the non-inertial co-rotating reference frame. To this end, the action S should be formulated in the curved background with the Euclidean metric corresponding to the co-rotating frame [39]:

$$g^E_{\mu\nu} = \begin{pmatrix} 1 & 0 & 0 & x_2\Omega_I \\ 0 & 1 & 0 & -x_1\Omega_I \\ 0 & 0 & 1 & 0 \\ x_2\Omega_I & -x_1\Omega_I & 0 & 1+x_\perp^2\Omega_I^2 \end{pmatrix} , \tag{12}$$

written in the Euclidean coordinates $x^\mu = (x^1, \ldots, x^4)$, where $x_4 = -it$ is the imaginary time coordinate and $x_\perp^2 = x_1^2 + x_2^2$. The system rotates around the x_3 axis.

The angular velocity in Eq. (12) is put in the purely imaginary form $\Omega_I = -i\Omega$ to avoid the sign problem [39]. The expressions for the Minkowski spacetime can be obtained by the analytical continuation. In particular, the velocity v_R at the boundary (4) becomes imaginary $v_I = -iv_R$, with the following relation:

$$v_I^2 = -v_R^2 . \tag{13}$$

The action in the co-rotating frame in the continuum Euclidean spacetime has the following form:

$$S = \frac{1}{4g^2} \int d^4x \sqrt{g_E}\, g_E^{\mu\nu} g_E^{\alpha\beta} F^a_{\mu\alpha} F^a_{\nu\beta} , \tag{14}$$

where $g^E_{\mu\nu} = (g_E^{\mu\nu})^{-1}$ is the curved Euclidean metric (12) with the determinant $g_E = \det(g_{\mu\nu}) = 1$ and $F^a_{\mu\nu}$ is the field strength of SU(3) gauge field.

Numerical first-principle results. We discretize rotating terms in the action (14) following Ref. [32, 39] and use the tree-level improved Symanzik gauge action for the terms without rotation [40, 41]. To set the temperature scale we use the results from Ref. [42].

Our calculations are performed on the lattices of size $N_t \times N_z \times N_s^2 = N_t \times 40 \times 41^2$ with $N_t = 5, 6, 7, 8$. We used periodic boundary conditions in all directions. For the zero temperature subtraction (11b) we use data from the lattice with the same spatial sizes and $N_t = 40$. The imaginary velocity at the boundary is identified with the velocity at the middle of the boundary side, $v_I = \Omega_I L_s/2$, where $L_s = a(N_s - 1)$ is the length of the lattice in the x and y directions. More details on numerical simulations can be found in Appendix.

In the inset of Fig. 1, we show the normalized difference of lattice action densities Δs (11b) which enters the free energy density (11a). At vanishing velocity of the rotation, $v_I = 0$, we recover the known result [38, 43]. The steep rise of Δs, which happens close to the critical coupling $\beta \simeq \beta_c$, points to the first order nature of the phase transition in the non-rotating plasma.

As the imaginary velocity v_I increases, the transition shifts towards smaller lattice couplings β signaling that the critical temperature $T_c = T_c(v_I)$ decreases as the *imaginary* angular frequency Ω_I (the velocity v_I of the rotation) raises. This result is in agreement with previous numerical calculations [31–33].

The normalized free energy density in the co-rotating frame, $-f/T^4$, calculated via Eq. (11a), is shown in Fig. 1. This quantity is a monotonically raising function of the temperature T at all imaginary velocities v_I, indicating the presence of a plateau at $T \to \infty$ for each fixed v_I.

The free energy density f, shown in Fig. 1, is a rising (diminishing) function of v_I^2 at fixed temperature $T < T_s$ ($T > T_s$). This property can be quantified by fitting of the free energy density at a fixed temperature T by a

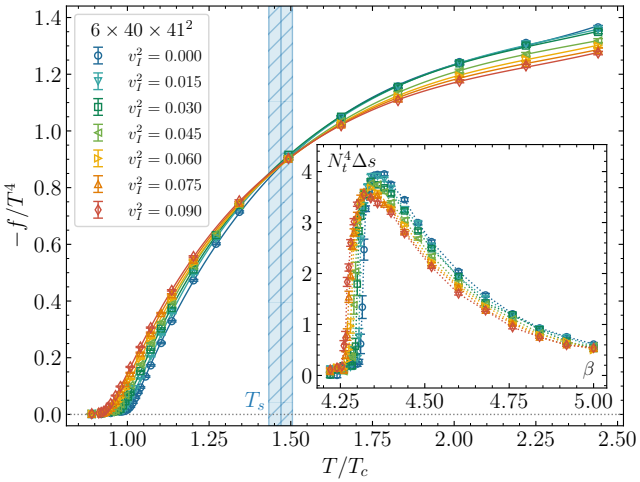

FIG. 1. The free energy density f in the co-rotating frame as a function of the temperature T for the $N_t = 6$ lattice. The vertical line shows the supervortical temperature T_s for this lattice. The inset shows the expectation value of the lattice action density Δs corresponding to the scale anomaly (11b) as a function of the lattice gauge coupling β. Both plots are given for several imaginary velocities squared v_I^2 at the boundary $R = L_s/2 \equiv 20a$ of the system, Eqs. (13) and (4), for the same lattice. Periodic boundary conditions are employed.

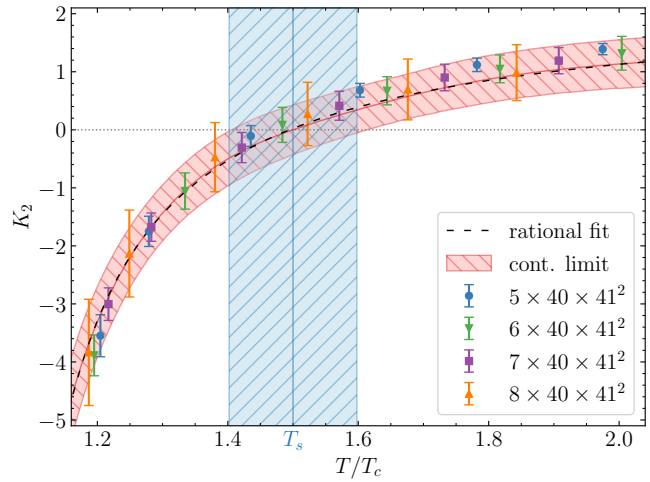

FIG. 2. The dimensionless moment of inertia K_2 of the gluon plasma as a function of the temperature T for several temporal lattice extensions N_t. The red shaded region, with the central values marked by the red solid line, denotes the continuum extrapolation, $K_2 = K_2^{(\text{cont.})} + C/N_t^2$ at $N_t \to \infty$ or, equivalently, $a \to 0$. The best fit (16) of the continuum curve is shown by the dashed black line. The position of the supervortical temperature T_s, extrapolated to continuum limit, is marked by the vertical line which separates the unstable ($T < T_s$) and stable ($T > T_s$) regimes of rigid plasma rotation. The error estimations (the shaded regions for T_s and $K_2^{(\text{cont.})}$, and the bars of the data) include both statistical and systematic uncertainties.

parabolic function

$$f(T, v_I) = f_0(T)\Big(1 - \frac{1}{2}K_2(T)v_I^2\Big)\,, \tag{15}$$

where f_0 and K_2 serve as fit parameters (we remind that $f_0 < 0$). The expression in the Euclidean spacetime (15) represents the first two terms of the free energy (7) in the co-rotating frame in the Minkowski spacetime after the Wick transformation for the boundary velocities (13). The dimensionless moment of inertia K_2 for several lattices and the corresponding continuum limit ($a \to 0$, or, equivalently, $1/N_t \to 0$ at a fixed temperature T) are shown in Fig. 2.

A striking feature of the free energy, Fig. 1, is that the curves corresponding to different v_I intersect at the same "supervortical" temperature T_s, signaling that at this temperature, the free energy (15) looses, at least for slow rotation $v_I^2 \ll 1$, the dependence on the rotational frequency. Therefore, the rigidly rotating gluon plasma looses its moment of inertia at $T = T_s$. We use this property as a definition of the supervortical temperature, $K_2(T_s) = 0$, and show its continuum limit in Fig. 2.

The continuum limit of the dimensionless moment of inertia can be well reproduced by a rational function

$$K_2^{(\text{fit})}(T) = K_2^{(\infty)} - \frac{c}{T/T_c - 1}\,, \tag{16}$$

where the best-fit parameters are the high-temperature asymptotics $K_2^{(\infty)} = 2.23(39)$ and the slope coefficient $c = 1.11(20)$. The high-temperature limit of the moment of inertia, $K_2^{(\infty)}$, is a non-universal quantity that may depend on the geometry of the rotating system and the boundary conditions.

In order to estimate systematic errors related to our determination of T_s, we repeat the whole procedure with several methods of numerical integration in Eq. (11a) and several upper limits $v_I^{(\max)}$ for the fit of the free energy density by the function (15). The final result for the lattices with periodic boundary conditions is given in Eq. (1), where the estimated uncertainty incorporates both statistical and systematic contributions.

As mentioned above, the absence of the massless excitations in the deconfinement phase implies the independence of our results on the type of boundary conditions in the transverse spatial directions, provided the spatial volume is large enough. To verify this property, we calculated the K_2 coefficient for the system with open boundary conditions and found an agreement with the periodic lattices, albeit more significant uncertainties. The corresponding supervortical temperature for the open system, $T_s/T_c = 1.53(15)$ agrees with the estimate for periodic boundary conditions (1).

(In)stability and sign of the moment of inertia. Formally, the negative moment of inertia, observed in the region of temperatures $T < T_s$, might imply that the rotation causes the quark-gluon plasma to cool down

(the faster rotation, the lower thermal energy). However, physically, this counter-intuitive effect, contradicting the kinematic Tolman-Ehrenfest picture [44, 45], indicates that the rigid rotation is impossible thermodynamically. The plasma experiences an instability which makes the rotation non-rigid. Similar instabilities occur in curved gravitational backgrounds of rotating Kerr and Myers-Perry black holes [7–9].

For a system in stable equilibrium at a given temperature T and angular velocity $\boldsymbol{\Omega}$, any deviation from the equilibrium should obey the following condition [37]:

$$\delta E - T\delta S - \boldsymbol{\Omega}\delta \boldsymbol{J} > 0\,, \tag{17}$$

which implies that all eigenvalues of the inverse Weinhold metric, defined in the thermodynamic space [46],

$$g^{(W),\mu\nu} = -\frac{\partial^2 f(T,\boldsymbol{\Omega})}{\partial X_\mu \partial X_\nu}\,, \qquad X_\mu = (T, \Omega_i)\,, \tag{18}$$

must be positively defined (see a discussion in [10]).

The positivity of the matrix (18) is achieved provided the specific heat at constant angular momenta C_J and the eigenvalues (spectrum) of the tensor of isothermal differential moment of inertia $I^{ij} \equiv I^{ji}$ are positive quantities:

$$C_J > 0\,, \qquad C_J = T\left(\frac{\partial S}{\partial T}\right)_J\,, \tag{19}$$

$$\mathrm{spec}(I^{ij}) > 0\,, \qquad I^{ij} = \left(\frac{\partial J^i}{\partial \Omega_j}\right)_T\,. \tag{20}$$

The inequality (19) is a standard requirement for the thermodynamic stability [37]. Given the cylindrical geometry of our system, the condition (20) reduces to the requirement $I > 0$ for the principal moment of inertia (3) at infinitesimally slow rotations, $\Omega \to 0$. In terms of the coefficient K_2, Eqs. (7) and (8), the thermodynamic stability requires:

$$K_2(T) > 0 \qquad \text{(thermodynamic stability)}, \tag{21}$$

which is violated below the supervortical temperature, $T < T_s$.

This instability has a thermodynamic origin. It has no obvious relation to the hydrodynamic instabilities that might be generated by the viscous flow of hot gluons.

Moment of inertia and scale anomaly. The moment of inertia I is directly related to the trace anomaly as one can see from Eqs. (8), (10), and (15):

$$I(T) = -T^4 \int_0^T \frac{dT'}{T'} \frac{\langle T^\mu_{\ \mu}\rangle^{(2)}(T')}{T'^4}\,, \tag{22}$$

where $\langle T^\mu_{\ \mu}\rangle^{(2k)}$ are the moments of the anomalous trace

$$\langle T^\mu_{\ \mu}\rangle^{(2k)}(T) = \frac{1}{(2k)!}\left[\frac{\partial^{2k}}{\partial v_I^{2k}}\langle T^\mu_{\ \mu}\rangle(T, v_I)\right]\Bigg|_{v_I=0}\,, \tag{23}$$

for $k \in \mathbb{Z}$. The equation (23) can readily be written for the real angular velocity using the correspondence (13).

Role of the magnetic gluon condensate. Using Eq. (3) or Eq. (20), we can derive, via a path-integral representation of Yang-Mills theory in a curved spacetime (14), the moment of inertia of gluons, $I \equiv I^{33}$:

$$I = I_{\rm fluct} + I_{\rm cond} = \int_V d^3x \int_V d^3x' \langle\!\langle M_0^{12}(\boldsymbol{x}) M_0^{12}(\boldsymbol{x}')\rangle\!\rangle_T + \int_V d^3x \langle\!\langle (\epsilon^{ij} F^a_{i3} x_j)^2 + (F^a_{12})^2 (x_1^2 + x_2^2)\rangle\!\rangle_T. \tag{24}$$

We used Eq. (5) and the relation $\Omega^2 = -\Omega_I^2$. In Eq. (24),

$$M^{ij}(\boldsymbol{x}) = x^i T^{j0}(\boldsymbol{r}) - x^j T^{i0}(\boldsymbol{x})\,, \qquad i,j = 1,2,3\,, \tag{25}$$

is the local angular momentum, which is related to the $\Omega \to 0$ limit of the stress-energy tensor of gluons:

$$T^{\mu\nu} = F^{a,\mu\alpha} F^{a,\nu}_{\ \ \alpha} - \frac{1}{4}\eta^{\mu\nu} F^{a,\alpha\beta} F^a_{\alpha\beta}\,. \tag{26}$$

We also used the notation $\langle\!\langle \mathcal{O}\rangle\!\rangle_T = \langle \mathcal{O}\rangle_T - \langle \mathcal{O}\rangle_{T=0}$ to denote the thermal part of the expectation value of an operator $\mathcal{O}$. The normalization of the moment of inertia (24) is chosen such that the cold vacuum has no inertia.

The first term in the moment of inertia (24) describes fluctuations of the angular momentum and has a standard linear-response form

$$I_{\rm fluct} = \langle\!\langle (J^3)^2\rangle\!\rangle_T, \qquad J^i = \frac{1}{2}\int_V d^3x\, \epsilon^{ijk} M^{jk}(\boldsymbol{x})\,, \tag{27}$$

were we used the fact that $\langle J^3\rangle = 0$ at $\Omega = 0$ at any temperature. One might expect that $I_{\rm fluct} > 0$ because thermal fluctuations always increase the susceptibility in addition to quantum fluctuations.

The second term in (24) involves a nonperturbative magnetic gluon condensate in the static, $\Omega \to 0$, limit. Using the $SO(3)$ rotational symmetry and the translational invariance of the plasma in spatial dimensions, we get the relation $\langle\!\langle F^a_{i3} F^a_{j3}\rangle\!\rangle_T = \delta_{ij}\langle\!\langle (F^a_{12})^2\rangle\!\rangle_T$, which can be expressed via the magnetic gluon condensate at a finite temperature $\langle\!\langle (F^a_{ij})^2\rangle\!\rangle_T \equiv 6\langle\!\langle (F^a_{12})^2\rangle\!\rangle_T$. We get:

$$I_{\rm cond} = \frac{1}{3}\int_V d^3x\, x_\perp^2 \langle\!\langle (F^2_{ij})^2\rangle\!\rangle = \frac{\pi}{6} L_z R^4 \langle\!\langle (F^a_{ij})^2\rangle\!\rangle_T\,. \tag{28}$$

Surprisingly, this relation has the same form as the classical formula for the moment of inertia (6), where the mass density ρ corresponds to the thermal part of the magnetic gluon condensate $\rho(T) = \langle\!\langle (F^a_{ij})^2\rangle\!\rangle_T/6$.

The full gluon condensate $\langle G^2\rangle$ (a sum of its electric and magnetic parts) is a phenomenologically important quantity which takes a positive value at $T = 0$ [47, 48]. It decreases monotonically with the increase of the temperature, implying that the thermal part of the condensate, $\langle\!\langle G^2\rangle\!\rangle_T$, always takes a negative value [49, 50]. This property, which is interpreted as melting of the gluon condensate, is in agreement with the relation of the thermal

condensate to the scale anomaly: $\langle\langle G^2\rangle\rangle_T = -\langle T^\mu_\mu\rangle_T < 0$ (see a discussion in Ref. [38]).

However, the magnetic contribution to the scale anomaly (11b) reverses its sign at $T \simeq 2T_c$ [38] indicating that the magnetic part of the thermal gluon condensate becomes positive and implying that $I > 0$ above $2T_c$. This effect is associated with the evaporation of the magnetic component of the gluon plasma [51, 52] and the associated string dynamics [51, 53]. Thus, the negative-valued condensate in $I_{\rm cond}$ should nullify the positive contribution of the correlator term $I_{\rm fluct}$ in a region below $2T_c$ in agreement with our estimate of the supervortical temperature (1), $T_s < 2T_c$.

In short, the thermal magnetic condensate takes a negative value right above T_c suggesting that the negative contribution of the condensate $I_{\rm cond}$ overwhelms the positive standard contribution $I_{\rm fluct}$ thus leading to a negative total moment of inertia (24), $I = I_{\rm fluct} + I_{\rm cond} < 0$, above T_c. At $T > T_s$, the perturbative hot gluons prevail the non-perturbative scale counterpart, and the moment of inertia becomes positive.

The suggested mechanism is also in a qualitative agreement with previous numerical observations indicating that *rigid* rotation increases the critical transition temperature T_c [31, 32]. Indeed, if the rigid rotation makes the plasma colder, then stronger thermal fluctuations (and, consequently, higher temperature) are needed to destroy the confinement phase in the rotating plasma as compared to the non-rotating plasma. This simple observation explains the effect of raising critical temperature T_c with increasing angular frequency Ω. Moreover, the crucial role of the magnetic condensate in our mechanism suggests that this effect should be absent for non-gluonic degrees of freedom. The latter hypothesis is perfectly consistent with the recent first-principle observation made, separately, for quarks and gluons in Ref. [33]

Our paper focuses on the investigation of pure gluon plasma, which exhibits the fundamental nonperturbative properties of its realistic quark-gluon counterpart. To clarify the contribution of quarks to the moment of inertia, we notice that Eq. (24) remains also valid in QCD. Namely, the total angular momentum M^{12} now includes not only the gluon part (25), but also the orbital, $\bar\psi\gamma_4(xD_y - yD_x)\psi$, and spin, $i/2\bar\psi\gamma_4\sigma_{12}\psi$, angular momenta of quarks. While the quark fields make a positive thermal contribution to the fluctuation term $I_{\rm fluct}$, the gluomagnetic contribution $I_{\rm cond}$ stays negative in QCD [54]. Following our discussions of gluon plasma, we conclude that $I \equiv I_{\rm fluct} + I_{\rm cond} < 0$ also for the quark-gluon plasma in a certain range of temperatures. Thus, we believe that the rigid rotation of quark-gluon plasma is also unstable in a certain temperature range around the transition temperature.

Conclusions. All *field-theoretical analytical and first-principle numerical* approaches dedicated to the investigation of the thermodynamics of rotating quark-gluon plasma consider a rigidly rotating plasma, meaning the angular velocity Ω at all points in the system, regardless of the distance to the rotational axis, takes the same value [55]. In other words, the plasma rotates like a solid body. While this assumption sounds unnatural from, at least, a hydrodynamic point of view (after all, the plasma is not a solid), the rigid rotation is very convenient in treating the system analytically. Moreover, the rigid approximation could sound reasonable for a sufficiently small, slowly rotating system as a first-order approximation to a more complicated, spatially inhomogeneous rotation.

In our work, we show that below the supervortical temperature (1), the rigid rotation of the gluon plasma is thermodynamically unstable even at slow rotation velocities. This effect exhibits a striking similarity with spinning black holes [7–11]. While the back-hole rotational instability is promoted by the curved gravitational background, the instability in the gluon plasma originates from the scale anomaly via the thermal part of the magnetic gluon condensate. Therefore, we conclude that the model of rigid rotation cannot be used, for thermodynamic reasons, for a realistic study of the rotation of the gluon plasma.

Our results also suggest that the puzzling discrepancy between numerical [31–33] and analytical (including holography [24], Tolman-Ehrenfest kinematic estimations [30], hadron-gas approach [25], and perturbative arguments [27] based on imaginary rotation [29]) models' predictions about the critical temperature in the center of rotating QCD (gluon) plasma might originate from the scale anomaly which should be taken into account appropriately. In particular, our work shows that the magnetic gluon condensate – which has a nonperturbative component at any temperature – plays a crucial role in rotating quark-gluon plasma.

Acknowledgments. The authors are grateful to Oleg Teryaev for useful discussions. This work has been carried out using computing resources of the Federal collective usage center Complex for Simulation and Data Processing for Mega-science Facilities at NRC "Kurchatov Institute", http://ckp.nrcki.ru/ and the Supercomputer "Govorun" of Joint Institute for Nuclear Research.

Appendix: Simulation details

We use the following lattice gluon action:

$$S_G = \beta \sum_x \Big((c_0 + r^2\Omega_I^2)(1 - \frac{1}{N_c}\mathrm{Re\ Tr}\ \bar{U}_{xy}) + (c_0 + y^2\Omega_I^2)(1 - \frac{1}{N_c}\mathrm{Re\ Tr}\ \bar{U}_{xz}) + \\ + (c_0 + x^2\Omega_I^2)(1 - \frac{1}{N_c}\mathrm{Re\ Tr}\ \bar{U}_{yz}) + c_0\big(3 - \frac{1}{N_c}\mathrm{Re\ Tr}\ (\bar{U}_{x\tau} + \bar{U}_{y\tau} + \bar{U}_{z\tau})\big) - \\ + \sum_{\mu\neq\nu} c_1(1 - \frac{1}{N_c}\mathrm{Re\ Tr}\ \bar{W}^{1\times 2}_{\mu\nu}) - \frac{1}{N_c}\mathrm{Re\ Tr}\ \big(y\Omega_I(\bar{V}_{xy\tau} + \bar{V}_{xz\tau}) - x\Omega_I(\bar{V}_{yx\tau} + \bar{V}_{yz\tau}) + xy\Omega_I^2\bar{V}_{xzy}\big)\Big), \quad (29)$$

where $\bar{U}_{\mu\nu}$ denotes the clover-type average of four plaquettes, $\bar{W}^{1\times 2}_{\mu\nu}$ is the rectangular loop, $\bar{V}_{\mu\nu\rho}$ is the asymmetric chair-type average of eight chairs [32], and $c_0 = 1-8c_1$, $c_1 = -1/12$. The action (29) in the case $c_1 = 0$ coincides with the lattice gauge action used in Refs. [31, 32].

For each lattice size we keep the (imaginary) angular velocity in lattice units unchanged with the variation of β, therefore, the linear velocity v_I at the boundary of the system remains constant with the changes in temperature. In our simulations the linear velocity takes the following values: $v_I^2 = 0.000, 0.015, 0.030, 0.045, 0.060, 0.075, 0.090$.

To set the temperature scale, we use the results for the string tension from Ref. [42]. For the non-rotating lattices with periodic boundary conditions, we use the values of the inverse critical coupling β_c taken from Ref. [42]. For the case of open boundary conditions, we determine β_c from the peak of the Polyakov loop susceptibility.

Simulations are performed using Monte Carlo algorithm, each sweep consists of one heatbath update and two steps of the overrelaxation updates. In finite (zero) temperature simulations typical statistics are about 5000-40000 (2000-10000) sweeps after thermalization for each set of parameters, depending on N_t of the finite temperature lattice. The statistical errors are estimated via the jackknife method.

* vvbraguta@theor.jinr.ru
† maxim.chernodub@univ-tours.fr
‡ roenko@theor.jinr.ru
§ sychev.da@phystech.edu

[1] L D Landau and E M Lifshitz, *Mechanics*, 3rd ed. (Butterworth-Heinemann, Oxford, England, 1982).

[2] Josip Lončar, Bojan Igrec, and Dubravko Babić, "Negative-inertia converters: Devices manifesting negative mass and negative moment of inertia," Symmetry **14**, 529 (2022).

[3] Wai-Kai Chen, ed., *The circuits and filters handbook, second edition*, 2nd ed., Circuits & Filters Handbook 3e (CRC Press, Boca Raton, FL, 2002).

[4] M. N. Chernodub, "Permanently rotating devices: extracting rotation from quantum vacuum fluctuations?" (2012), arXiv:1203.6588 [quant-ph].

[5] M. N. Chernodub, "Rotating Casimir systems: magnetic-field-enhanced perpetual motion, possible realization in doped nanotubes, and laws of thermodynamics," Phys. Rev. D **87**, 025021 (2013), arXiv:1207.3052 [quant-ph].

[6] Antonino Flachi and Matthew Edmonds, "Quantum vacuum, rotation, and nonlinear fields," Phys. Rev. D **107**, 025008 (2023), arXiv:2212.02776 [hep-th].

[7] Bernard F Whiting and James W York Jr, "Action principle and partition function for the gravitational field in black-hole topologies," Physical Review Letters **61**, 1336 (1988).

[8] Tim Prestidge, "Dynamic and thermodynamic stability and negative modes in schwarzschild–anti-de sitter black holes," Physical Review D **61** (2000), 10.1103/physrevd.61.084002.

[9] Harvey S. Reall, "Classical and thermodynamic stability of black branes," Physical Review D **64** (2001), 10.1103/physrevd.64.044005.

[10] Ricardo Monteiro, Malcolm J. Perry, and Jorge E. Santos, "Thermodynamic instability of rotating black holes," Phys. Rev. D **80**, 024041 (2009), arXiv:0903.3256 [gr-qc].

[11] Natacha Altamirano, David Kubizňák, Robert Mann, and Zeinab Sherkatghanad, "Thermodynamics of rotating black holes and black rings: Phase transitions and thermodynamic volume," Galaxies **2**, 89–159 (2014).

[12] L. Adamczyk *et al.* (STAR), "Global Λ hyperon polarization in nuclear collisions: evidence for the most vortical fluid," Nature **548**, 62–65 (2017), arXiv:1701.06657 [nucl-ex].

[13] Francesco Becattini and Michael A. Lisa, "Polarization and Vorticity in the Quark–Gluon Plasma," Ann. Rev. Nucl. Part. Sci. **70**, 395–423 (2020), arXiv:2003.03640 [nucl-ex].

[14] Xu-Guang Huang, Jinfeng Liao, Qun Wang, and Xiao-Liang Xia, "Vorticity and Spin Polarization in Heavy Ion Collisions: Transport Models," Lect. Notes Phys. **987**, 281–308 (2021), arXiv:2010.08937 [nucl-th].

[15] Victor E. Ambruş and Elizabeth Winstanley, "Rotating quantum states," Phys. Lett. B **734**, 296–301 (2014), arXiv:1401.6388 [hep-th].

[16] Victor E. Ambrus and Elizabeth Winstanley, "Rotating fermions inside a cylindrical boundary," Phys. Rev. D **93**, 104014 (2016), arXiv:1512.05239 [hep-th].

[17] Hao-Lei Chen, Kenji Fukushima, Xu-Guang Huang, and Kazuya Mameda, "Analogy between rotation and density for Dirac fermions in a magnetic field," Phys. Rev. D **93**, 104052 (2016), arXiv:1512.08974 [hep-ph].

[18] Yin Jiang and Jinfeng Liao, "Pairing Phase Transitions of Matter under Rotation," Phys. Rev. Lett. **117**, 192302 (2016), arXiv:1606.03808 [hep-ph].

[19] M. N. Chernodub and Shinya Gongyo, "Interacting fermions in rotation: chiral symmetry restoration, moment of inertia and thermodynamics," JHEP **01**, 136 (2017), arXiv:1611.02598 [hep-th].

[20] M. N. Chernodub and Shinya Gongyo, "Effects of rotation and boundaries on chiral symmetry breaking of

relativistic fermions," Phys. Rev. D **95**, 096006 (2017), arXiv:1702.08266 [hep-th].

[21] Xinyang Wang, Minghua Wei, Zhibin Li, and Mei Huang, "Quark matter under rotation in the NJL model with vector interaction," Phys. Rev. D **99**, 016018 (2019), arXiv:1808.01931 [hep-ph].

[22] Zheng Zhang, Chao Shi, Xiao-Tao He, Xiaofeng Luo, and Hong-Shi Zong, "Chiral phase transition inside a rotating cylinder within the Nambu–Jona-Lasinio model," Phys. Rev. D **102**, 114023 (2020), arXiv:2012.01017 [hep-ph].

[23] N. Sadooghi, S. M. A. Tabatabaee Mehr, and F. Taghinavaz, "Inverse magnetorotational catalysis and the phase diagram of a rotating hot and magnetized quark matter," Phys. Rev. D **104**, 116022 (2021), arXiv:2108.12760 [hep-ph].

[24] Xun Chen, Lin Zhang, Danning Li, Defu Hou, and Mei Huang, "Gluodynamics and deconfinement phase transition under rotation from holography," JHEP **07**, 132 (2021), arXiv:2010.14478 [hep-ph].

[25] Yuki Fujimoto, Kenji Fukushima, and Yoshimasa Hidaka, "Deconfining Phase Boundary of Rapidly Rotating Hot and Dense Matter and Analysis of Moment of Inertia," Phys. Lett. B **816**, 136184 (2021), arXiv:2101.09173 [hep-ph].

[26] Anastasia A. Golubtsova, Eric Gourgoulhon, and Marina K. Usova, "Heavy quarks in rotating plasma via holography," Nucl. Phys. B **979**, 115786 (2022), arXiv:2107.11672 [hep-th].

[27] Shi Chen, Kenji Fukushima, and Yusuke Shimada, "Perturbative Confinement in Thermal Yang-Mills Theories Induced by Imaginary Angular Velocity," Phys. Rev. Lett. **129**, 242002 (2022), arXiv:2207.12665 [hep-ph].

[28] Anastasia A. Golubtsova and Nikita S. Tsegel'nik, "Probing the holographic model of $\mathcal{N} = 4$ SYM rotating quark-gluon plasma," (2022), arXiv:2211.11722 [hep-th].

[29] M. N. Chernodub, "Inhomogeneous confining-deconfining phases in rotating plasmas," Phys. Rev. D **103**, 054027 (2021), arXiv:2012.04924 [hep-ph].

[30] M. N. Chernodub, V. A. Goy, and A. V. Molochkov, "Inhomogeneity of rotating gluon plasma and Tolman-Ehrenfest law in imaginary time: lattice results for fast imaginary rotation," (2022), arXiv:2209.15534 [hep-lat].

[31] V. V. Braguta, A. Yu. Kotov, D. D. Kuznedelev, and A. A. Roenko, "Study of the Confinement/Deconfinement Phase Transition in Rotating Lattice SU(3) Gluodynamics," Pisma Zh. Eksp. Teor. Fiz. **112**, 9–16 (2020).

[32] V. V. Braguta, A. Yu. Kotov, D. D. Kuznedelev, and A. A. Roenko, "Influence of relativistic rotation on the confinement-deconfinement transition in gluodynamics," Phys. Rev. D **103**, 094515 (2021), arXiv:2102.05084 [hep-lat].

[33] V. V. Braguta, A. Yu. Kotov, A. A. Roenko, and D. A. Sychev, "Thermal phase transitions in rotating QCD with dynamical quarks," in *39th International Symposium on Lattice Field Theory* (2022) arXiv:2212.03224 [hep-lat].

[34] Andreas Athenodorou and Michael Teper, "The glueball spectrum of su(3) gauge theory in 3 + 1 dimensions," Journal of High Energy Physics **2020**, 172 (2020).

[35] I.e., pressure does not depend on the combination $\Omega/\Lambda_{\rm QCD}$.

[36] Hereafter, subleading terms in angular frequency Ω are neglected.

[37] L D Landau and E M Lifshitz, *Statistical Physics*, 3rd ed. (Butterworth-Heinemann, Oxford, England, 1996).

[38] G. Boyd, J. Engels, F. Karsch, E. Laermann, C. Legeland, M. Lutgemeier, and B. Petersson, "Thermodynamics of SU(3) lattice gauge theory," Nucl. Phys. B **469**, 419–444 (1996), arXiv:hep-lat/9602007.

[39] Arata Yamamoto and Yuji Hirono, "Lattice QCD in rotating frames," Phys. Rev. Lett. **111**, 081601 (2013), arXiv:1303.6292 [hep-lat].

[40] G. Curci, P. Menotti, and G. Paffuti, "Symanzik's Improved Lagrangian for Lattice Gauge Theory," Phys. Lett. B **130**, 205 (1983), [Erratum: Phys.Lett.B 135, 516 (1984)].

[41] M. Luscher and P. Weisz, "Computation of the Action for On-Shell Improved Lattice Gauge Theories at Weak Coupling," Phys. Lett. B **158**, 250–254 (1985).

[42] B. Beinlich, F. Karsch, E. Laermann, and A. Peikert, "String tension and thermodynamics with tree level and tadpole improved actions," Eur. Phys. J. C **6**, 133–140 (1999), arXiv:hep-lat/9707023.

[43] Sz. Borsanyi, G. Endrodi, Z. Fodor, S. D. Katz, and K. K. Szabo, "Precision SU(3) lattice thermodynamics for a large temperature range," JHEP **07**, 056 (2012), arXiv:1204.6184 [hep-lat].

[44] Richard Tolman and Paul Ehrenfest, "Temperature Equilibrium in a Static Gravitational Field," Phys. Rev. **36**, 1791–1798 (1930).

[45] Richard C. Tolman, "On the Weight of Heat and Thermal Equilibrium in General Relativity," Phys. Rev. **35**, 904–924 (1930).

[46] F. Weinhold, "Metric geometry of equilibrium thermodynamics," The Journal of Chemical Physics **63**, 2479–2483 (1975).

[47] Mikhail A. Shifman, A. I. Vainshtein, and Valentin I. Zakharov, "QCD and Resonance Physics. Theoretical Foundations," Nucl. Phys. B **147**, 385–447 (1979).

[48] Mikhail A. Shifman, A. I. Vainshtein, and Valentin I. Zakharov, "QCD and Resonance Physics: Applications," Nucl. Phys. B **147**, 448–518 (1979).

[49] David E. Miller, "The Gluon condensate in QCD at finite temperature," Acta Phys. Polon. B **28**, 2937–2947 (1997), arXiv:hep-ph/9807304.

[50] Philipp Gubler and Daisuke Satow, "Recent Progress in QCD Condensate Evaluations and Sum Rules," Prog. Part. Nucl. Phys. **106**, 1–67 (2019), arXiv:1812.00385 [hep-ph].

[51] M. N. Chernodub and V. I. Zakharov, "Magnetic component of Yang-Mills plasma," Phys. Rev. Lett. **98**, 082002 (2007), arXiv:hep-ph/0611228.

[52] Jinfeng Liao and Edward Shuryak, "Magnetic Component of Quark-Gluon Plasma is also a Liquid!" Phys. Rev. Lett. **101**, 162302 (2008), arXiv:0804.0255 [hep-ph].

[53] L. Ya. Glozman, "Chiral spin symmetry and hot/dense QCD," (2022), arXiv:2209.10235 [hep-lat].

[54] M. Ishii and T. Hatsuda, "Hadronic screening masses and the magnetic gluon condensate at high temperature," Phys. Lett. B **338**, 319–324 (1994), arXiv:hep-ph/9408209.

[55] Exceptions in the literature are not known to the authors.